

Instrumented Tensile Adhesion Tests on Plasma Sprayed Thermal Barrier Coatings

Christopher C. Berndt

Abstract. Tensile adhesion tests (TATs) which are normally utilized for industrial quality control procedures have been used for research purposes to examine failure mechanisms of plasma sprayed coatings. This work is applied to two layer coatings (NiCrAlY or NiCrAlZr bond coat with a yttria stabilized zirconia ceramic overlay) which are tested in tension perpendicular to the surface. The mechanical behavior of the bond coat and ceramic overlay were not measured separately. However, the specific component of the coating which sustains the major deformation is related to the failure locus and enables an empirical determination of the bond coat and ceramic overlay deformations to be postulated.

It has been determined that adhesive failure within the bond coat exhibits greater failure strain than cohesive failure of the ceramic overlay. This view lends support to the commonly accepted understanding of these intermediate coatings being highly compliant. The absolute extension exhibited by failures which occur only through the ceramic coating (i.e., cohesive failure) is greater than that of adhesive failure because the ceramic coating is much thicker than the bond coat.

The stress vs. extension data can be expressed in terms of stress vs. strain, and hence the modulus of the coating components approximated to be about 100 MPa. This value is several orders in magnitude lower than that previously reported in the literature and the technical reasons for this discrepancy are discussed.

INTRODUCTION

Tensile adhesion test (TAT) methodology [1] has application in measuring the bond strength of thermally sprayed coatings. The bond strength which is determined by this means is highly variable [2] for any nominally identical group of coatings and can not be relied on as being indicative of the true material property of adhesion. It is appropriate for the TAT to be critically examined since this property, among others, is used to assess the relative merits of candidate coatings during the early stages of their development.

There are two major shortcomings of the TAT. Of prime importance is that the precise forces are not known throughout the deformation of the coating, and that these primarily tensile forces may bear little relationship to the biaxial compression and radial tension forces which are exerted on the coating during

its service life [3] as a thermal barrier coating. Another test feature is that the fracture mode may be atypical of that exhibited by coatings during their service life, and the value of tests whereby the failure mechanism is not reproduced can be questioned. In a like fashion there is often variability in the fracture modes of nominally identically prepared TAT specimens [4].

A TAT procedure was adopted in the present study despite these shortcomings with the intention of focussing on the coating deformation. In this fashion the structure/property relationships of coatings which were intended for thermal barrier applications were investigated.

INSTRUMENTED TENSILE ADHESION TESTS

Materials and Method

The U-700 alloy specimens were in the shape of a pproximately 13 mm radius disks which were 6 mm thick and with an edge radius of 3 mm. The disk shape

The author is with the Department of Materials Engineering, Monash University, Clayton, Victoria, Australia. 3168.

of the specimen facilitated the application of a two-layer coating system over its entire surface of 20.6 cm². This geometry also enabled two TATs to be performed on each specimen. The bond coat material was either NiCrAlY (i.e., Y active) or NiCrAlZr (i.e., Zr active) and 0.13 mm thick. The ceramic overlay was of ZrO₂-8 wt.%Y₂O₃ and nominally 0.38 mm thick. Two different bond coat materials were used to produce coatings which would be expected to have different mechanical properties. Some of the coatings were also subjected to heat treatment at 1150°C to further enhance differences in their behavior. Table 1 summarizes the various types of coatings and their heat treatment conditions. The results which are included in this table will be discussed later.

The pull-off bar was manufactured from mild steel and had a contact diameter of 25.4 mm against the coated specimen. The adhesive, Scotchweld, was cured at 110°C for 70 min. An alignment jig was manufactured so that the coating surface and bonding portion of the pull-off bar could be precisely held in a parallel orientation during the curing cycle. It should be noted, in passing, that the most recent develop-

ment with regard to TAT specimen preparation is to use an aerospace thin film adhesive which is known as FM73 (a 3M product). This adhesive is quite easy to handle and permits the various components of the specimen to be easily aligned [4]. A pull-off ring was incorporated into the specimen assembly prior to the gluing procedure. The pull-off ring enabled a tensile force to be applied to the coating.

Standard tensile adhesion testing procedure does not measure the specimen extension since only the load at failure is required to calculate the failure stress. However, in these tests the extension was accurately measured with two clip gauges which were positioned on opposite sides of the specimen (Fig. 1). Knife edges, in the form of cut up blades, were glued to the pull-off ring and the pull-off bar so that the clip gauges could be attached. The average extension between both clip gauges was used to calculate the gross extension of the specimen.

Compliance Calibration

The mechanical properties, as measured above, include the deformation of the coating, epoxy, sub-

Table 1. Summary of Specimen Heat Treatments and Test Data¹

Specimen Code	Active Bond Coat Species	Number of 1 Hour Cycles	Failure Mode ^b	Failure Stress (×10 ⁶ Pa)	Failure Extension (×10 ⁻⁶ m)	Gradient (×10 ⁹ Pa m ⁻¹)
07B	Y	0	e	19.8	34.8	526
24A	Y	0	m	18.5	1.6	9156
08B	Y	0	e	17.6	176.5	101
24B	Y	0	a2	16.7	22.0	821
40B	Y	0	m	15.8	19.7	855
07A	Y	0	a2	15.4	22.0	700
08A	Y	0	a2	14.1	117.7	113
40A	Y	0	m	13.6	36.2	321
33B	Y	8	a2	11.9	21.2	458
33A	Y	8	a2	11.4	7.9	1113
17A	Y	22	a2	8.8	15.1	483
17B	Y	22	a2	7.5	24.3	340
16A	Zr	0	a1	15.4	12.7	1420
32A	Zr	0	a1	15.4	48.3	266
16B	Zr	0	a1	11.4	36.9	324
32B	Zr	0	a1	10.5	18.1	585
09A	Zr	6	c	14.9	42.1	349
41B	Zr	6	c	12.7	42.8	273
25A	Zr	6	c	11.9	60.0	197
25B	Zr	6	c	11.4	24.9	447
09B	Zr	6	c	10.1	36.9	260
41A	Zr	6	c	7.9	27.0	290

The adjustment for the compliance calibration has been carried out on a point-for-point basis (refer to the text).

^a1—adhesive (substrate/bond coat)

a2—adhesive (bond coat)

c—cohesive

m—mixed mode

e—epoxy

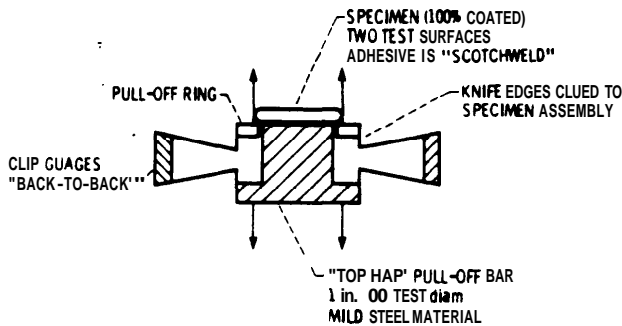


Fig. 1. Schematic of tensile adhesion test apparatus. The two clip gauges are attached between a collar (which fits around the coated specimen) and the pull-off bar (which is glued to the coating).

strate, and pull-off bar. The deformation of the components which are not related to the coating system can be measured on an uncoated specimen which is solely used for the purpose of calibrating the system. Seven specimens were tested in this manner and Figure 2 shows a plot of the stress versus average extension for these calibration specimens. Figure 2 also shows the maximum and minimum values of extension at each stress level to present the accuracy of the compliance calibration. The absolute accuracy of the average compliance curve is about 30% of the experimental range of all observations. However, when a measure for central tendency, such as the standard deviation, is used as an error measurement then the accuracy of the compliance curve is about $\pm 15\%$ for stress levels greater than 5 MPa.

During testing the specimen assembly was first loaded to about 400 N to allow "bedding-in" of the specimen into the fixtures. The specimen was then unloaded to about 250 N so that it would remain aligned with respect to the tensile axis. At this stage the two clip gauges were readjusted to zero and then the specimen loaded to failure. Therefore, it may be observed that the stress/extension curve for the average compliance calibration does not pass through the origin (Fig. 2).

The load/extension properties of the uncoated specimen can be subtracted from the mechanical properties which are exhibited by the coated specimen. Therefore, the mechanical properties of coating as well as any thermal-processing-induced effects upon the substrate were ascertained. The compliance curve approximates a straight line. However, significant errors can evolve if the compliance subtraction is carried out by assuming this fit, especially at low stresses where a slight change in curve shape can be observed (Fig. 2). Therefore, the compliance data was subtracted from the tensile adhesion test data on a point-for-point basis, for up to 47 points, in intervals of

222.7 N (i.e., 50 lb). It is most likely that the failure stress will not occur at an integral value of the force interval, and therefore the last value of the compliance curve was interpolated by assuming a linear fit between the end point values of the compliance data. The final correction to the stress/extension data concerns translating the data to suit zero force at the origin. It should be emphasized that the stress/extension data presented in this paper have been manipulated by the methods described above and thus represent the properties of only the coating or any thermal-processing-induced effects upon the substrate.

RESULTS

Twenty-two tensile adhesion tests were carried out and a summary of the stress/extension results is presented in Table 1. The fracture morphology was determined by examination of the specimen surfaces with the unaided eye and follows the terminology illustrated in Figure 3. The primary failure modes of interest may be defined as cohesive and adhesive. Adhesive failure occurs either within the bond coat (type 2) or at the interface between the substrate and bond coat (type 1). Cohesive failure occurs entirely within the ce-

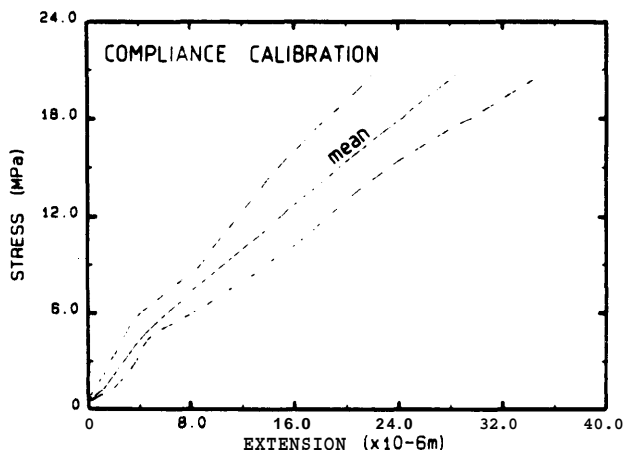


Fig. 2. Compliance calibration data for tensile adhesion test specimens. The average compliance; as well as the minimum and maximum values for 7 uncoated specimens is shown.

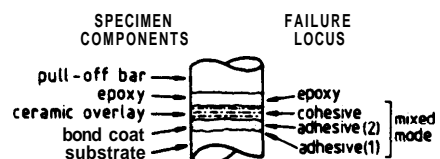


Fig. 3. Schematic of failure mode descriptions.

ramic coating, and mixed mode failure is defined as a combination of the adhesive and cohesive modes.

The stress/extension data of each TAT approximately fitted a straight line. The minimum correlation coefficient (R^2) was 0.84 but was more typically above 0.95. The slope of the stress/extension plot is directly proportional to the modulus of the coating. The precise numerical value of this modulus can only be determined if the deformation zone of the coating in response to the applied force is known. Thus, since the coating strain cannot be ascertained with the information presented so far, then the gradients of the stress/extension data will be initially examined with a view to studying trends between the various coatings. The probability plot of these gradients (Fig. 4) reveal a bimodal distribution such that high values correspond to adhesive failure, low values to cohesive failure, and mixed mode failure is distributed over the entire range of gradient values. There is some overlap in the failure morphology with respect to the gradient of the stress/extension curve, and such trends are quite common for mechanical property measurements on thermally sprayed coatings. The stress/extension data which exhibited the three lowest gradient values for cohesive failure and the three largest values for adhesive failure are shown in Figure 5 to illustrate these extreme cases in failure morphology.

The two types of coatings examined had a ZrO_2 -8 wt% Y_2O_3 overlay deposited onto either a bond coat of NiCrAlY or NiCrAlZr. It is common experience that plasma sprayed coatings degrade on being subjected to thermal environments [5]. Therefore, it might also be expected for their mechanical properties to change. The properties of the coating change because of bond coat oxidation which alters the stress pattern within the coating. This aspect of modifying the coating characteristics was studied by selecting several specimens for heat treatment at 1150° C prior to tensile adhesion testing. It was established that the failure mode, after heat treatment, was different for each

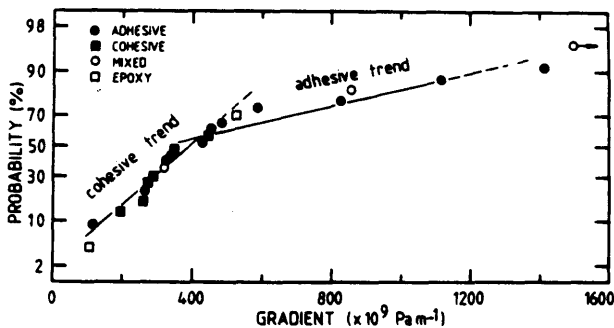


Fig. 4. Probability plot of gradient values for stress/extension data of plasma sprayed coatings.

bond coat; being adhesive (type 2) for the Y-active bond-coat (77.7Ni-16Cr-6Al-0.3Y in wt.%) and cohesive for the Zr-active (71.9Ni-14Cr-14Al-0.1Zr) bond coat. The data envelopes for each failure mode are indicated in Figure 6.

The major emphasis of the present work is to determine whether different failure modes are representative of different material properties. Figures 5 and 6 show that cohesive failure modes are generally 'more compliant' (i.e., extension/force is greater) than adhesive failure modes if the deformation is assumed to occur over the entire coating thickness. Therefore, the cohesive failure mode of the coating system exhibited a lower modulus than adhesive failure. The limited data (3 points only) for mixed mode failure encompasses both the adhesive and cohesive strength/extension fields; depending on the precise contribution of each failure mode, and this is indicated by a dashed curve which covers both of these fields.

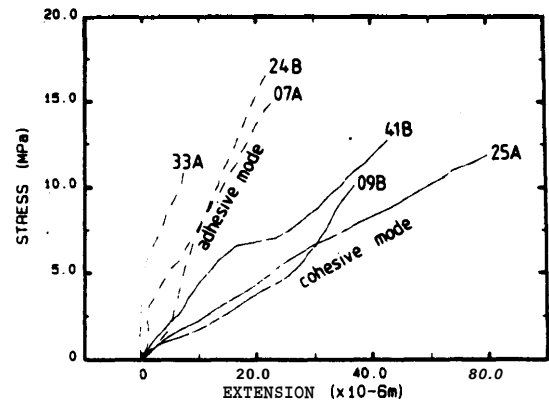


Fig. 5. Stress/extension plots of tensile adhesion tests to illustrate adhesive and cohesive modes of failure.

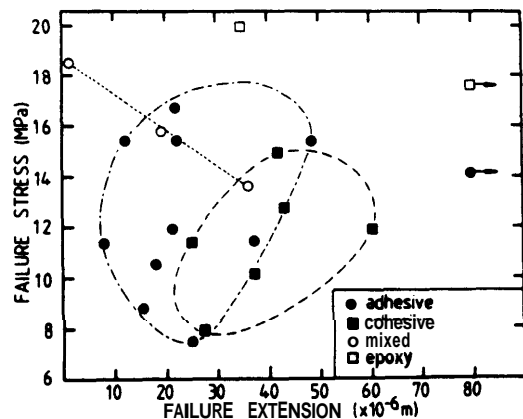


Fig. 6. Failure stress versus failure extension data for NiCrAlY + ZrO_2 -8 wt.% Y_2O_3 and NiCrAlZr + ZrO_2 -8 wt.% Y_2O_3 plasma sprayed coatings. The data envelopes for the various failure modes are indicated.

DISCUSSION

This work presents methods for the accurate determination of the **stress/extension** behavior of duplex systems of plasma sprayed coatings which are subjected to tensile stresses **perpendicular** to the substrate surface. It is necessary to carry out a reliable compliance calibration and the best way of using this calibration is by a direct point-for-point subtraction from the tensile adhesion test data. The reproducibility of the compliance data is satisfactory and has a relative accuracy of about 15% about the mean value. The **error** range could most probably be decreased by careful monitoring of the epoxy thickness, but this extra precaution was not warranted in the case of the present study.

One major point to remember is that the tensile adhesion test data has been pooled for both types of bond coats and for the various pretreatment conditions of the coating system. Both aspects of the coating formulation were varied to promote different failure modes and these were observed to belong to different distributions (Fig. 6) although there was some overlap. Not too much emphasis can be placed on the failure stress, at least for the purposes of the present study, because of the variable nature of coating preparation and the limited results in terms of replicate tests.

The **stress/extension** data was used to establish representative values of the gradient for each mode of failure. The gauge lengths for adhesive, cohesive, and mixed mode failure has been taken as the thicknesses of the bond coat (0.13 mm), ceramic coating (0.38 mm), and coating system (0.51 mm), respectively. Therefore, the modulus for the coating in tension may be found (Table 2). It should be emphasized that the data reported in this work has support from similar studies [6] where **stress/extension** gradients from 250 to 3120 Pa m⁻¹ were obtained for zirconia-8 wt% yttria coatings. (Note that these results are not reported in Reference [6] but can be calculated from the data presented in that report.)

Determination of the Modulus

The values of modulus shown in Table 2 are averages for each failure mode. This modulus has been cal-

culated by using **stress/extension** data which includes plastic deformation of the coating. It would be expected that coatings which are subjected to low stress levels (say <2 MPa) would also exhibit no permanent extension on unloading. Therefore, the tangent modulus at low stresses is equivalent to an elastic modulus. It was observed that this gradient increases, especially for the adhesive and mixed mode types of failure. The maximum modulus which has been determined by this means is 4.7 GPa, and this value is within an order of magnitude to that of about 20 GPa which has been found for alumina plasma sprayed coatings (7,8). It should be emphasized that the modulus value of 4.7 GPa was determined by assuming that deformation occurred throughout the thickness of the coating (taken as 0.51 mm).

The point of the preceding discussion is that it is necessary to know the strain in order to calculate the modulus of the coating. When the strain over the entire coating is homogeneous then the coating thickness is used in this calculation. However, if there is a preferred plane (or a material volume of several lamellae in thickness) over which deformation occurs then the true strain may be quite large and therefore the modulus is low.

The elastic modulus for plasma sprayed coatings of ZrO₂-24 wt% MgO has also been determined as 46.2 GPa [9,10]. However, this value is an average of two tests and the variability of the results is not known. Other factors which make direct comparison of results difficult are that the coating was of a different composition than the one used in this study, the coating was removed from the substrate prior to testing, and a four-point bending method was used to test the coatings. There is a change in the stress sign about the neutral axis in this test and the compressive strength of the coating will contribute to the Young's modulus determination. These coatings also exhibited significant acoustic emission at forces about one-half of the ultimate failure stress during loading, and this is direct evidence of cracking within the coating—most probably on the tension side of the four-point bend specimen.

The modulus of the ceramic coatings used in this study are significantly less than values determined by other means. The reason for this is that the present tests were performed in pure tension and calculations were **carried** out over the entire elastic and plastic range of deformation. The tangent modulus, which would suit an elastic analysis, exhibited values within an order of magnitude of other studies. Cohesive failure exhibited a linear **stress/extension** relationship, but this does not imply elastic deformation. In fact no specimens in this study were unloaded before failure to establish the precise **elastic/plastic** nature of the

Table 2. Mechanical Properties of Coatings

Failure Mode	Gradient (Pa m ⁻¹)	Component Deformation	Thickness of Layer (mm)	Modulus (MPa)
Adhesive	660	Bondcoat	0.13	86
Cohesive	300	Ceramic overlay	0.38	115
Mixed mode	630	Bondcoat + ceramic overlay	0.51	32

specimen deformation. However, a similar study [6] has verified that there is a net extension, which suggests plastic deformation, when the tensile adhesion specimen is unloaded prior to failure. Thus the elastic modulus at low stress levels [8] or under conditions where there is a complex tension/compression stress pattern [10] is greater than the modulus found in this work where there is almost pure tension. The choice of which modulus to consider as characteristic of the coating depends on the service conditions imposed on the particular coating. The modulus, as established in this work, may define the observed coating behavior at high stresses more precisely than a modulus which is based on elastic deformation.

The low values of modulus correlate to a high compliance for these coatings. Thus, there may be considerable deformation without an apparent change in coating integrity during stressing. This feature of the coating mechanical behavior has been demonstrated by bending substrates, to which a plasma sprayed ceramic coating has been applied, to almost U-shaped configurations with little spalling of the coating [11]. The physical picture of the coating mechanical behavior to explain the above observations is one where the lamellae slide over each other yet still remain interlocked into the coating structure. Therefore, the coating would exhibit a nonlinear stress/strain (or stress/extension) curve and significant microcracking prior to catastrophic failure. However, the experiment of bending a coated substrate applies a force parallel to the interface between the coating and the substrate, and is quite unlike the force conditions during a TAT.

Finally, it should be remembered that the modulus of the coating components were calculated on the assumption that the failure locus gave a crude indication of the gauge length of the material under test. This model may not apply, in which case the values calculated represent lower limits of the modulus since deformation probably occurred over the entire coating thickness.

Cracking Processes in Coatings

A simple model of the coating structure is shown in Figure 7, where the three-dimensional interlaced lamellar network of the flattened particles coexists with cracks which are oriented either parallel or perpendicular to the substrate surface. Under the conditions of a TAT it would be expected that delamination cracking would be the dominant mode of deformation since the interlamellar region is a large area of microstructural nonuniformity. It is also reasonable to assume that the ultimate locus of failure indicates the prime region of the coating system which is undergoing deformation.

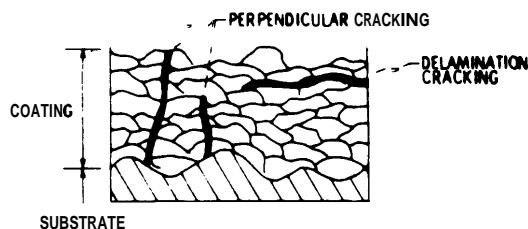


Fig. 7. Schematic diagram of a coating cross section which exhibits various cracking features.

Thus it can be thought that the coating strength may be improved by increasing the specific surface area of contact between adjoining lamellae. This concept of improving the mechanical properties of thermally sprayed coatings has some support. For example, previous work [12] attributed increased cohesive strength to small particles which had melted, or larger particles which had partially melted, and flowed around protuberances on unmelted particles (Fig. 8). The acoustic emission tests on high-strength coatings qualitatively confirmed such a model by registering a large proportion of high count rates. This is thought to be indicative of many microcracks occurring around the protuberances of unmelted particles and the surface morphology of the particle will greatly influence any mechanism of this nature. Particles with a low surface area to volume ratio will not exhibit this mode of cohesion. Other work [13] has examined methods of enhancing the coating toughness via the encorporation of a second phase so that a composite-type structure can be manufactured.

The terms which are used in the following discussion should be defined. The "strain" exhibited by the coating is directly related to its 'deformation.' It may include both elastic and plastic deformation processes. A high strain infers a large compliance as well

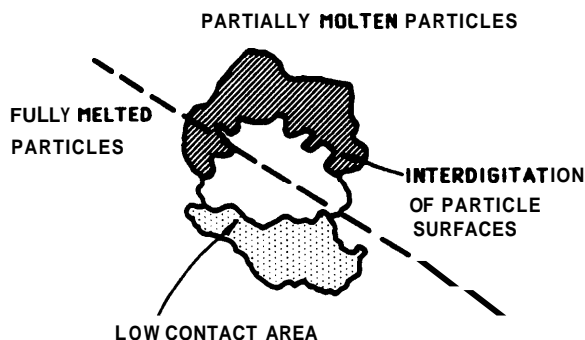


Fig. 8. Schematic diagram of lamellae interactions which lead to either (i) a highly adherent interface with interdigitation of particle surfaces of (ii) poor adhesion from low contact area.

as a **low** modulus. The converse is **true** for a low strain. 'Cracking' phenomena may occur in **response** to deformation processes. The stress at which cracking processes are initiated is usually regarded as the maximum operating stress for an engineering component. Materials which exhibit a high modulus are termed as 'brittle' and exhibit low strains prior to cracking and failure. A final point to remember is that the mechanical and material properties of thermally sprayed coatings have never been related to the same properties of the respective bulk materials.

It is useful to formulate some physical models for the coating deformation during the adhesive and cohesive modes of failure. The models presented in this work are intended to promote a mechanistic understanding of coating deformation processes during TATs. The bond coat is approximately one-third the thickness of the ceramic overlay. Deformation processes during adhesive failure are concentrated in this layer since, by definition, this is the ultimate locus of failure. Acoustic emission studies [6] also indicate that much less cracking phenomena occur during this deformation mode than for cohesive failure. Additional evidence from fractographic analysis of TAT specimens (this work, as well as Reference [4]) and mode I fracture toughness tests [14] has shown that adhesive failure of bond coats exhibits significant lamellae deformation compared to cohesive failures of ceramic coatings.

The foregoing suggests that a simple picture of adhesive failure is of significant lamellae deformation which is influenced by a crack network. Cohesive failure (Fig. 9), on the other hand, shows a higher density of internal cracking as well as edge cracking which would be expected from stress concentration effects [15,16]. The current model additionally proposes that, since the lamellae deformation mechanism of the bond coat is greater than that of the ceramic overlay, then the strain exhibited by adhesive failure must be greater than that of cohesive failure. Thus, the strain is maximized within the bond coat during the adhesive mode of failure. Such a mechanism also correlates well with the current understanding of bond coats as acting as compliant layers between the ceramic overlay and metallic substrate.

It should be further noted that the strain of adhesive failure (i.e., failure extension divided by the coating thickness) has been **reasoned** to be greater than that of cohesive failure. However, the absolute extension during cohesive failure is greater than that during adhesive failure (Fig. 5). The above discussion and conclusions have been indirectly corroborated by other workers [10] as follows. The modulus ("E" in their terminology) for the ceramic overlay of a similar coating system was determined to be **20 GPa** and the

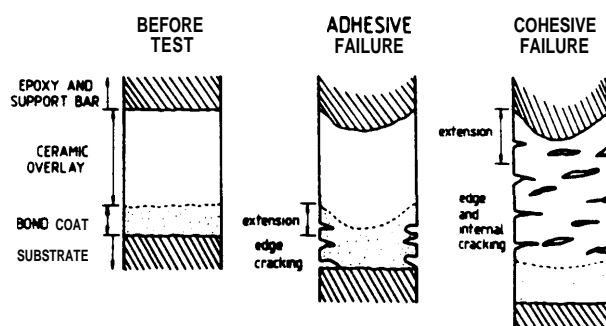


Fig. 9. Schematic diagram to illustrate the coating deformation response during the adhesive and cohesive failure modes. The bond coat and ceramic coating features of the TAT are drawn to scale in the longitudinal direction only to indicate where deformation of the coating is most prominent. The deformation of the support bar and coating is exaggerated. Refer to text for further details.

failure stress was about **19 MPa**. The E for the bond coat was **200 GPa** and the failure stress (at the yield point) was **1000 MPa**. If the approximation of a linear stress vs. strain response is made, then the failure strains of the ceramic overlay and bond coat can be approximated to **0.085%** and **0.50%**, respectively, confirming that strain during adhesive failure (not necessarily the absolute extension) is concentrated to the bond coat.

Figure 9 illustrates that the total extension of the coating is greatest for the cohesive failure mode (in accordance with the experimental data, Fig. 5), even though the ceramic component is the stiffest (i.e., higher modulus) part of the **coating/substrate** system, because the ceramic coating is normally at least three times thicker than the metallic bond coat. The methods described in this work also show that instrumented TAT techniques allow mechanistic aspects of coating behavior to be examined; and herein lies a powerful research tool to understand thermal spray coating properties.

CONCLUDING REMARKS

Two broad classifications of tests have been discussed in this paper. The TAT may be used either as a routine quality control procedure or, on the other hand, as a research tool and, as such, provide information with regard to the physico-mechanical behavior of thermally sprayed coatings. It is possible to bridge these industrial and research methods by use of an appropriate statistical analysis so that a scientific understanding of coating performance can be obtained.

A method for the precise measurement of the material properties of plasma sprayed coatings has been detailed. The properties of the coating have been de-

terminated by accounting for the deformation behavior of any components of the specimen which are not directly associated with the coating.

The **stress/extension** behavior of coating systems was determined and the gradients of these curves were found to be characteristic of the failure mode. Adhesive failure (failure in or including the bond coat) exhibited a gradient of about $660 \text{ GPa } m^{-1}$ and cohesive failure (failure within the ceramic) a value of $300 \text{ GPa } m^{-1}$. Mixed mode failure generally displayed values which overlapped both the adhesive and cohesive distributions. The **stress/extension** data was approximated to **stress/strain** data by assuming that deformation was constrained mostly to the plane of failure. In this way the modulus was determined to be from 32 to 115 **MPa**. It should be emphasized that this modulus is fundamentally different from an elastic modulus because the coating system is deformed plastically—at least on a microscale between adjoining lamellae. Thus, coatings which exhibit good adhesion may plastically deform rather than resist the stresses and maintain their original structure like a high modulus, defect-free material.

ACKNOWLEDGMENTS

This work was supported by NASA-Lewis Research Center (Cleveland, OH, USA) under cooperative agreement NCC3-27; and under a Research Fellowship awarded by Monash University (Melbourne, Australia). The author would like to thank his colleagues at these Institutions for their contributions and support. Special thanks go to Associate Professor R. McPherson (Monash University), Professor H. Herman (SUNY at Stony Brook), and Dr. R.A. Miller (NASA-Lewis Research Center) for their helpful discussions during my residence at their respective institutions. The author also wishes to thank the reviewers for their constructive criticism.

REFERENCES

1. ASTM C633-69: 'Standard Method for Adhesion or Cohesive Strength of Flame-Sprayed Coatings,' American Society for Testing and Materials, Philadelphia, 1969.
2. F.J. Hermanek: 'Determining the Adhesive Cohesive

Strength of Thin Thermally Sprayed Deposits." *Weld J.*, 1978, Vol. 57, pp. 31–35.

3. R.A. Miller and C.E. Lowell: 'Failure Mechanisms of Thermal Barrier Coatings Exposed to Elevated Temperatures,' *Thin Solid Films*, 1982, Vol. 95, pp. 265–274.
4. P. Ostojic and C.C. Berndt: 'The Variability in Strength of Thermally Sprayed Coatings,' *Surface and Coatings Technology*, 1988, Vol. 34, pp. 43–50.
5. R.A. Miller: 'Oxidation-Based Model for Thermal Barrier Coating Life,' *Am. Ceram. Soc. J.*, 1984, Vol. 67, No. 8, pp. 517–521.
6. R.M. Shankar, C.C. Berndt, and H. Herman: 'Characterization of the Mechanical Properties of Plasma-Sprayed Coatings,' *Mater. Sci. Res.*, 1983, Vol. 15, pp. 473–490.
7. P. Boch, D. Fargeot, C. Gault, and F. Platon: 'Variations of the Elastic Moduli of Alumina during Structural Phase Transition,' *Rev. Int. Hautes Temper. et Refract.*, 1981, Vol. 18, pp. 85–93.
8. J.C. Glandus, F. Platon, and P. Boch: 'Measurements of the Elastic Moduli of Ceramics,' *Materials in Engineering Applications*, 1979, Vol. 1, pp. 243–246.
9. P.A. Siemers and R.L. Mehan: 'Mechanical and Physical Properties of Plasma Sprayed Stabilized Zirconia,' *Ceram. Eng. Sci. Proc.*, 1983, Vol. 4, No. 9–10, pp. 828–840.
10. P.A. Siemers and W.B. Hillig: "Thermal-Barrier-Coated Turbine Blade Study," Final Report, NASA CR-165351, August, 1981, 123 pages.
11. R.C. Hendricks, G. McDonald, and R.L. Mullen: "Residual Stress in Plasma-Sprayed Ceramic Turbine and Gas-Path Seal Specimens," *Ceramic Eng. and Sci. Proc.*, 1983, Vol. 4, No. 9–10, pp. 802–809.
12. N.R. Shankar, C.C. Berndt, and H. Herman: 'Failure and Acoustic Emission Response of Plasma-Sprayed ZrO_2 -8 wt% Y_2O_3 ,' *Ceram. Eng. Sci. Proc.*, 1982, Vol. 3, No. 9–10, pp. 772–792.
13. C.C. Berndt and Y.H. Yi: "The Manufacture and Microstructure of Fiber Reinforced Thermally Sprayed Coatings," *Surface Coatings and Technology*, 1989, Vol. 37, pp. 89–110.
14. C.C. Berndt and R. McPherson: 'The Adhesion of Plasma Sprayed Ceramic Coatings to Metals,' *Mater. Sci. Res.*, 1981, Vol. 14, pp. 619–628.
15. P.C. Hopman: 'The Direct Pull-Off Test,' *JOCCA*, 1984, Vol. 7, pp. 179–184.
16. J. Sickfeld: "Pull-Off Test, an Internationally Standardized Method for Adhesion Testing—Assessment of the Relevance of Test Results." pp. 543–567 *Adhesion Aspects of Polymeric Coatings*, K.L. Mittal (Ed.), Plenum, New York, 1983.